Acta Polytechnica CTU Proceedings **33**:58–62, 2022
https://doi.org/10.14311/APP.2022.33.0058

Published by the Czech Technical University in Prague

DURABILITY OF GFRP CONNECTORS UNDER SUSTAINED COMPRESSION LOAD FOR USE IN SANDWICH WALLS

Stefan Carstens*, Matthias Pahn

Technische Universität Kaiserslautern, Department of Civil Engineering, Erwin-Schrödinger-Straße 52, 67663 Kaiserslautern, Germany

* corresponding author: stefan.carstens@bauing.uni-kl.de

Abstract. Precast concrete sandwich panels are used to fulfil the rising thermal requirements. The sandwich walls consist of three layers, a facing, a thermal insulation layer, and a load bearing layer. The two outer layers are coupled by connectors made of glass-fibre reinforced polymer. A lack of knowledge about load-bearing behaviour prevents the removal of sustained compressive loads. In the context of this article, tests under sustained compressive load are presented. To represent closely the in service-conditions of sandwich walls, the examined connectors were subjected to a saturated alkaline concrete environment as well as to a specified stress level till failure occurs. Thus, the experimental setup combines alkaline resistance and creep rupture tests into one comprehensive testing. By using temperature effects as an accelerating factor, reasonable test durations were enabled. The obtained time to failure line was determined to extrapolate the characteristic values of the long-term strength for a service life up to 50 years. The test results are compared and evaluated with existing test results under a sustained tensile load.

Keywords: Durability, GFRP connector, sandwich wall sustained compression load.

1. Introduction

Precast concrete sandwich panels have been used as exterior wall systems for many years and have proven themselves in practice [1]. They are characterised by numerous design options (Fig. 1) as well as high resistance to weathering and ageing [2]. The prefabricated wall elements have a three-layer structure consisting of a facing layer, a factory-installed thermal insulation layer, and a load-bearing layer. In standard cases, the facing and load-bearing layers are made of normal concrete [3] and in individual cases of lightweight concrete [4] or high-performance concrete [5]. The facing layer serves as an architectural design element that is at least 70 mm thick [6] and fulfils the function of weather protection for the thermal insulation material. The load-bearing layer performs load-bearing functions and is at least 140 mm thick. The thermal insulation materials used are expanded polystyrene (EPS) according to DIN EN 13163 [7], extruded polystyrene (XPS) according to DIN EN 13164 [8], and insulation materials based on polyurethane (PUR) according to DIN EN 13165 [9]. Usual insulation thicknesses are between 60 to 240 mm.

Discrete connectors made of corrosion-resistant materials are used to connect the facing and the load bearing layer [6]. These must allow deformations of the facing layer due to thermal effects as free as possible from constraining forces and simultaneously transfer wind and dead-loads across the thermal insulation [10]. To avoid thermal bridges, metallic connectors such as stainless-steel connectors are increasingly being replaced by connectors made out of fibre-reinforced plastic (FRP). The connectors usually consist of a thermosetting plastic matrix and unidirectional reinforcing glass fibres.

Figure 1. Precast concrete sandwich panels for use as a façade [5].

The individual components perform different tasks within the composite [11]. The fibres used are thin ($\varnothing\,3\ldots25$ mm), unidirectional oriented continuous glass fibres, which are completely enclosed by a synthetic resin matrix. Due to their mechanical properties, the inorganic fibres have a decisive influence on the stiffness and strength of the composite material [12]. Thermosetting polymers such as epoxy resins (EP), vinyl ester resins (VE), and vinyl ester urethane resins (VEU) are mainly used as materials for the synthetic resin matrix. The matrix fixes the fibres in the desired geometric position, transfers the stress between the fibres, prevents the fibres from buckling under a compressive load, and protects the fibres from external mechanical and chemical stress.

The advantages of the individual components are combined by the interaction of the glass fibre and the polymer matrix. In addition to the properties of the components and their proportions, pultrusion

Name		Isolink	ThermoPin	TM-MC Anchor
Matrix material		VEU	EP	VE
Fibre material	wt. %	87.1	n/a	74.0
	vol. %	74.3	n/a	53.0
Surface		ripped	wound	flat
Min. tensile strength	N/mm^2	1.000	1.500	700
Tensile Young's modulus	N/mm^2	60.000	60.000	40.000
Section dimensions	mm	$\varnothing_c$ 12.0; $\varnothing_e$ 13.5	$\varnothing_e$ 7.3	h/w 9.8/5.7

TABLE 1. Characteristics of GFRP Connectors acc. to [13].

[12] and the specific interaction of matrix resin and reinforcing fibre are decisive for the properties of the composite material.

Connectors made of glass-fibre reinforced plastic differ significantly in terms of material composition and cross-sectional geometry. Table 1 gives an overview of the material and geometry characteristics of different GRP connectors.

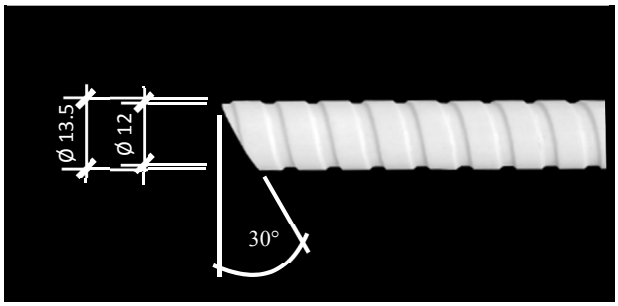

FIGURE 2. The geometry of the examined connector's head made out of glass fibre reinforced polymers.

In the further course of this paper, the Isolink [14] shown in Figure 2 will be considered as the connector for sandwich wall elements. The connector has a core diameter of 12 mm made out of glass fibre reinforced polymers. The total diameter of the connector, core, and ribs, is 13.5 mm. The ribs are made by indented trapezoidal thread with a profile depth of 0.6 to 0.75 mm and a pitch of 8 mm. The ends of the connector are bevelled at an angle of 30°.

In addition to temporary loads due to wind and temperature effects, the connectors must also be withstanding permanent loads due to the dead load of the facing layer. Loads acting vertically on the facing layer are carried by horizontally arranged anchors. The dead load of the facing layer is transferred using load-bearing anchor systems consisting of horizontal and diagonal anchors.

The support anchor system consisting of horizontal and diagonal anchors and the associated static system for calculating the distribution of forces in the support anchor system under the dead load of the facing layer are shown in Figure 3. As a result of the force-deflection, tensile forces arise in the diagonal connector $N_{t,sust}$ and compressive forces in the horizontal connector $N_{c,sust}$ which have a permanent effect.

2. Load-bearing behaviour under short-term compression load

While the load-bearing behaviour of the connectors under short-term [15] and long-term tension load [16] is known, there is a lack of knowledge about the load-bearing behaviour under compressive load, especially the stability load-bearing behaviour under consideration of exposures (humidity, temperature and alkalinity). In the context of this paper, therefore, the results of experimental investigations into the load-bearing behaviour under compressive load with large insulation thicknesses are presented. During the test, the connectors are subjected to short-term and long-term pressure loads.

In evaluate the load-bearing behaviour under short-term compressive loading, compression tests were carried out at insulation thickness of 160 mm, 250 mm, 300 mm and 350 mm [17]. The specimen geometry is shown in Figure 4. To ensure a realistic anchorage of the connectors in the facing and load bearing layer, the connectors are embedded in normal concrete. The thickness of each concrete layer is 120 mm, the other cross-sectional dimensions are 300 × 300 mm. The core layer consists only of the connector, no thermal insulation is used.

The test specimen is loaded during the test procedure using a servo-hydraulic test cylinder controlled by displacement. The transverse speed is 0.5 mm/min. Simultaneously, the force is measured using a load cell and the deformation through inductive displacement transducers. The determined loads are shown in Figure 5. With an insulation thickness of 160 mm, the connectors fail locally in the clamping area combined on thrust and pressure. With other insulation thicknesses, an interlaminar shear crack occurs over the entire length of the connector.

Furthermore, Figure 5 shows the recalculation of the stability tests according to equation 1. A double-sided clamping of the connector is assumed (Euler Case IV, K = 0.5). The second moment of inertia is using the core diameter $\varnothing_c = 12$ mm without considering a stabilizing effect of the ribs.

$$P_{cr} = \frac{\pi^2 EI}{(KL)^2} \tag{1}$$

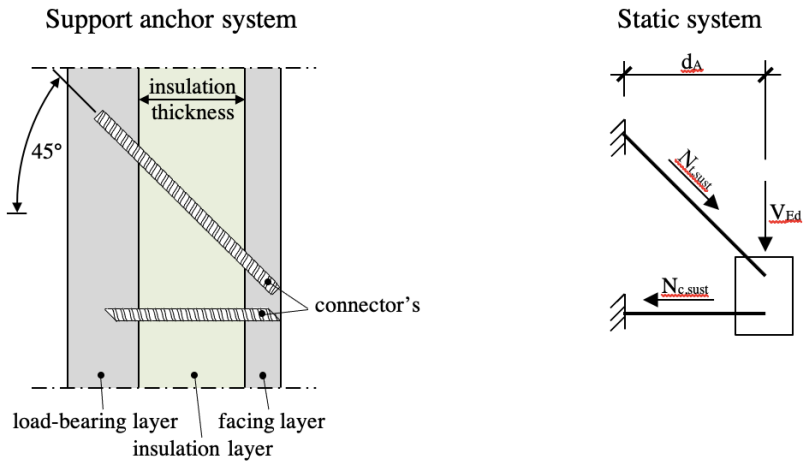

Figure 3. Support anchor system (left) and static system (right) to calculate the distribution of forces in the support anchor system due to the dead load of the facing layer V_{Ed}.

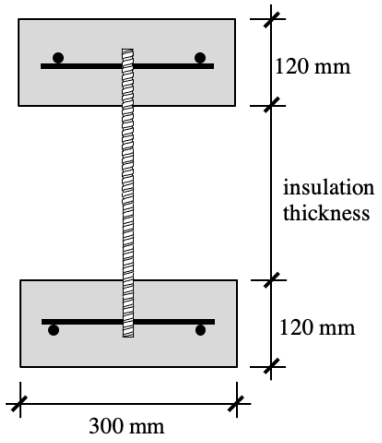

Figure 4. Geometry of the test specimens for short- and long-term tests under compression load.

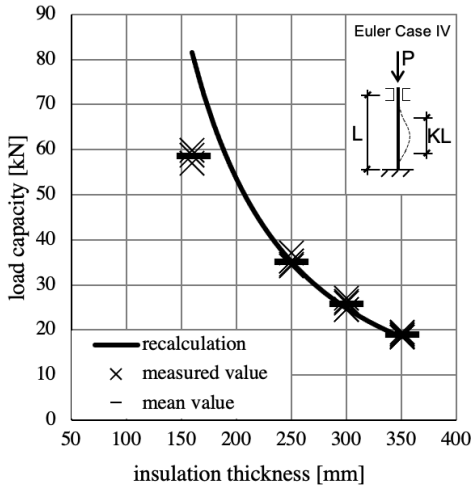

Figure 5. Experimentally and numerically determined the load-bearing capacity of the connector under compression load as a function of the insulation thickness.

It can be shown that the results of the experimental investigations for the insulation thicknesses 250 mm, 300 mm and 350 mm correspond very well with the recalculation. With an insulation thickness of 160 mm, the load-bearing capacity is overestimated by the recalculation. The reason for this is the change in the failure mode described above.

3. Experimental investigation under sustained compression load

The mechanical and physical properties of the composite material can degrade over time due to physical effects from e.g. creep and environmental influences. Since the transfer of the dead load of the facing layer must be ensured over the entire service life of the façade, these influences must be taken into account when determining permissible load-bearing capacities. The connectors are particularly exposed to temperature and humidity. Furthermore, the alkalinity of the concrete can damage the matrix.

To evaluate the load capacity of the connectors under compressive load, creep tests to failure are carried out to determine the respective service life.

3.1. Experimental set-up and execution of experiments under sustained load

The test setup for the creep tests is shown in Figure 6. The test specimens described above are placed in a tempered water bath. The water level reaches to just below the upper edge of the lower concrete abutment. The water is held at 60 řC to simulate increased surfaced temperatures in the area of the façade. The increased temperature causes water vapour to form, which settles on the connector and loads to a moderate moisture load.

The force is applied by a centrally arranged hydraulic cylinder. The hydraulic pressure in the cylin-

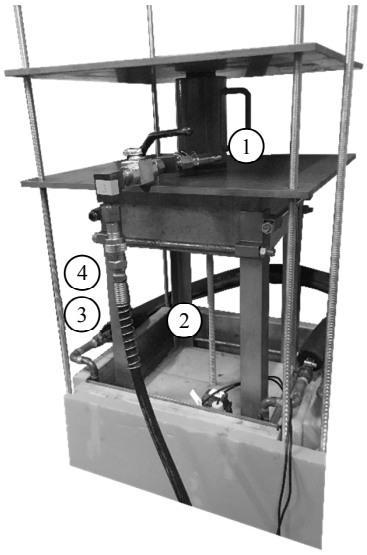

FIGURE 6. Experimental set-up for compression tests under continuous load and exposure to humidity, temperature and alkalinity; 1 hydraulic jack and oil pressure sensor; 2 test specimen; 3 temperature regulation; 4 stainless-steel profiles for guiding the specimen.

der is applied by a manual hydraulic pump and measured by an oil pressure sensor. The deformations of the specimen are measured simultaneously by an inductive displacement transducer. The concrete abutments of the test specimens are guided in parallel by a stainless-steel construction to prevent later deflections.

3.2. Results of experimental investigations under sustained load

The time-deformation diagram in Figure 7 shows the course of the deformation over the load duration. The three technical creep ranges are marked. The elastic deformation of the test specimen can be seen at the beginning. In the initial area, the test specimen shows an increase in linear deformation (primary creep area). The test specimen is then subjected to constant creep (secondary creep). This is followed by an increasing creep deformation (tertiary creep) which is finally followed by the failure of the test specimen.

Compared to the load capacity of 18.9 kN shown in Figure 5, a reduction of the load capacity to 16 kN can be determined for a service life of approximately 100 h. This reduction is probably due in particular to the influence of temperature and humidity.

3.3. Evaluation of the results of experimental investigations

Further service lives are achieved by varying the loads. Figure 8 shows the previous service lives of running and finished tests and the associated loads. With decreasing load, an increase in service life is expected. From the service lives of the individual tests

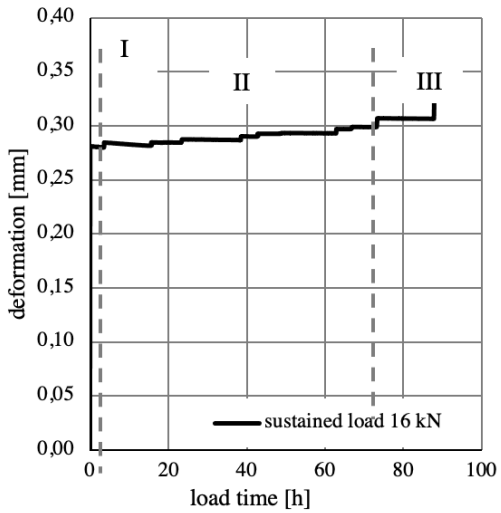

FIGURE 7. Deformation of the test specimen over the test period at an insulation thickness of 350 mm.

and loads, a permissible load for the intended service life of 50 years is then to be derived by extrapolation. The extrapolation should be performed according to [18]. The calculated load capacity for an insulation thickness is on the safe side as insulation thicknesses range from 60 to 350 mm.

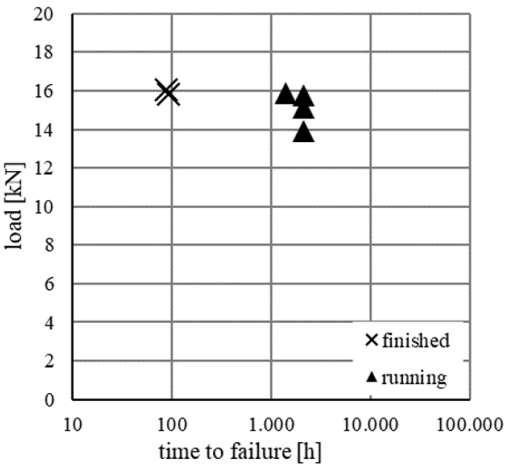

FIGURE 8. Load - time to failure diagram of creep tests at an insulation thickness of 350 mm.

4. Conclusions

Multilayer concrete sandwich panels have been used as exterior wall systems for many years and have been proven themselves in practice. Connectors made of glass fibre reinforced polymers are increasingly being used to couple the concrete layers. To transfer the dead load of the facing layer through a support anchor system consisting of connectors, the connectors must permanently absorb compressive loads.

In this paper, experimental investigations under short-term and long-term compression load are presented. It can be shown that the tests with insulation

thicknesses between 250 and 350 mm can be recalculated very well using the Euler equation. In the long-term tests, an increased influence of temperature and humidity on the failure load can be derived from the initial results. Finally, a concept for extrapolation is proposed for the determination of permissible load capacities.

Acknowledgements

The authors thank Schöck Bauteile GmbH for the financial and technical support provided.

References

[1] M. Pahn. Beitrag zur Ermittlung von Schnitt- und Verformungsgrößen bei mehrschichtigen Stahlbetonwandtafeln mit Verbindungsmitteln aus glasfaserverstärktem Kunststoff Kaiserslautern Germany, Ph.D. thesis, Kaiserslautern, Deutschland, 2011.

[2] R. Gastmeyer. Neuentwicklungen bei der Konstruktion mehrschichtiger Stahlbeton-Wandtafeln mit integrierter Wärmedämmung. *Beton- und Stahlbetonbau* **98**(6):360-8, 2003. https://doi.org/10.1002/best.200301750.

[3] M. Pahn, J. Schnell. Einfluss der Verbundtragwirkung bei mehrschichtigen Stahlbetonwandtafeln mit innen liegender Wärmedämmung. *Beton- und Stahlbetonbau* **106**(8):551-60, 2011. https://doi.org/10.1002/best.201100040.

[4] F. Hanz. Beitrag zur Bemessung von dreischichtigen Wandtafeln mit Deckschichten aus haufwerksporigem Leichtbeton Kaiserslautern, Ph.D. thesis, Kaiserslautern (Deutschland), 2017.

[5] F. Müller, C. Kohlmeyer, J. Schnell. Sandwichelemente mit Deckschichten aus Hochleistungsbeton und einem Kern aus extrudiertem Polystyrol. *Beton- und Stahlbetonbau* **110**(12):799-810, 2015. https://doi.org/10.1002/best.201500038.

[6] DIN EN 1992-1-1/NA 2013. Nationaler Anhang - National festgelegte Parameter - Eurocode 2: Bemessung und Konstruktion von Stahlbeton- und Spannbetontragwerken - Teil 1-1: Allgemeine Bemessungsregeln und Regeln für den Hochbau, 2013.

[7] EN 13163 2016. Thermal insulation products for buildings - Factory made expanded polystyrene (EPS) products - Specification, 2016.

[8] EN 13164 2015. Thermal insulation products for buildings - Factory made extruded polystyrene (XPS) products - Specification, 2015.

[9] EN 13165 2016. Thermal insulation products for buildings - Factory made rigid polyurethane foam (PU) products - Specification, 2016.

[10] P. Bindseil. Stahlbeton Fertigteile nach Eurocode 2 - Konstruktion, Berechnung, Ausführung, *Werner Verlag*, 2012.

[11] A. Schumann, M. May, M. Curbach. Carbonstäbe im Bauwesen. Beton- und Stahlbetonbau 113(12):868-76, 2018. https://doi.org/10.1002/best.201800077.

[12] H. Schürmann. Konstruieren mit Faser-Kunststoff-Verbunden, *Springer Verlag*, 2017.

[13] DAfStb 615 (en). Commentary to EN 1992-4 - Design of Fastenings for use in Concrete, 2019.

[14] Zulassung Z-21.8-1894. Schöck Isolink für mehrschichtige Betontafeln, 2018. https://www.dibt.de/de/service/zulassungsdownload/detail/z-218-1894.

[15] F. Micelli, A. Nanni. Mechanics of Composite Materials 39(4):293-304, 2003. https://doi.org/10.1023/a:1025638310194.

[16] M. L. Keller, M. Pahn. Durability of GFRP Bars with Different Bar Diameters. IABSE Symposium, Guimaraes 2019: Towards a Resilient Built Environment Risk and Asset Management, p.603-10, 2019. https://doi.org/10.2749/guimaraes.2019.0603.

[17] Bericht 06046Pa/528. Untersuchungen zur Eignung von ComBAR - Hohlwandankern aus glasfaserverstärktem Kunststoff als Verbindungselement von kerngedämmten Wänden mit aufstehender Vorsatzschale unreleased Bericht 10012Pav/14511 2015 Versuche zur Bestimmung des Widerstandes gegen Stabilitätsversagen von Schöck Thermoankern (unreleased), 2008.

[18] A. Weber. Prüfkonzepte für Bewehrungsmaterialien mit zeitabhängigen Widerständen Bauingenieur, 2018.